Supplementary Materials: Synthesis, Characterization and Biological Evaluation of Red-Absorbing Fe(II) Polypyridine Complexes

Johannes Karges, Philippe Goldner and Gilles Gasser

Table of Content:

Figure S1. ^{1}H NMR spectrum of **4** in CD_3CN, 400 MHz S2

Figure S2. ^{13}C NMR spectrum of **4** in CD_3CN, 100 MHz. S2

Figure S3. ESI-HRMS spectrum of **4** (positive detection mode). S3

Figure S4. ^{1}H NMR spectrum of **5** in CD_3OD, 400 MHz. S3

Figure S5. ^{13}C NMR spectrum of **5** in CD_3OD, 100 MHz. S4

Figure S6. ESI-HRMS spectrum of **5** (negative detection mode). S4

Figure S7. ^{1}H NMR spectrum of **6** in CD_3OD, 400 MHz. S5

Figure S8. ^{13}C NMR spectrum of **6** in CD_3OD, 100 MHz. S5

Figure S9. ESI-HRMS spectrum of **6** (negative detection mode). S6

Figure S10. Normalised Emission Spectrum of **4** in CH_3CN. S6

Figure S11. Normalised Emission Spectrum of **5** in CH_3CN. S7

Figure S12. Normalised Emission Spectrum of **6** in CH_3CN. S7

Figure S13. HPLC chromatogram of Caffeine (internal standard) and **4** after 0 and 48 h incubation in human pooled plasma. S8

Figure S14. HPLC chromatogram of Caffeine (internal standard) and **5** after 0 and 48 h incubation in human pooled plasma. S8

Figure S15. HPLC chromatogram of Caffeine (internal standard) and **6** after 0 and 48 h incubation in human pooled plasma. S8

Figure S16. Temporal change of the UV/Vis spectra of $[Ru(bipy)_3]Cl_2$ by irradiation at 450 nm in CH_3CN. S9

Figure S17. Temporal change of the UV/Vis spectra of **4** by irradiation at 450 nm in CH_3CN. S9

Figure S18. Temporal change of the UV/Vis spectra of **5** by irradiation at 450 nm in CH_3CN. S10

Figure S19. Temporal change of the UV/Vis spectra of **6** by irradiation at 450 nm in CH_3CN. S10

Figure S20. Temporal change of the UV/Vis spectra of PpIX by irradiation at 450 nm in CH_3CN. S11

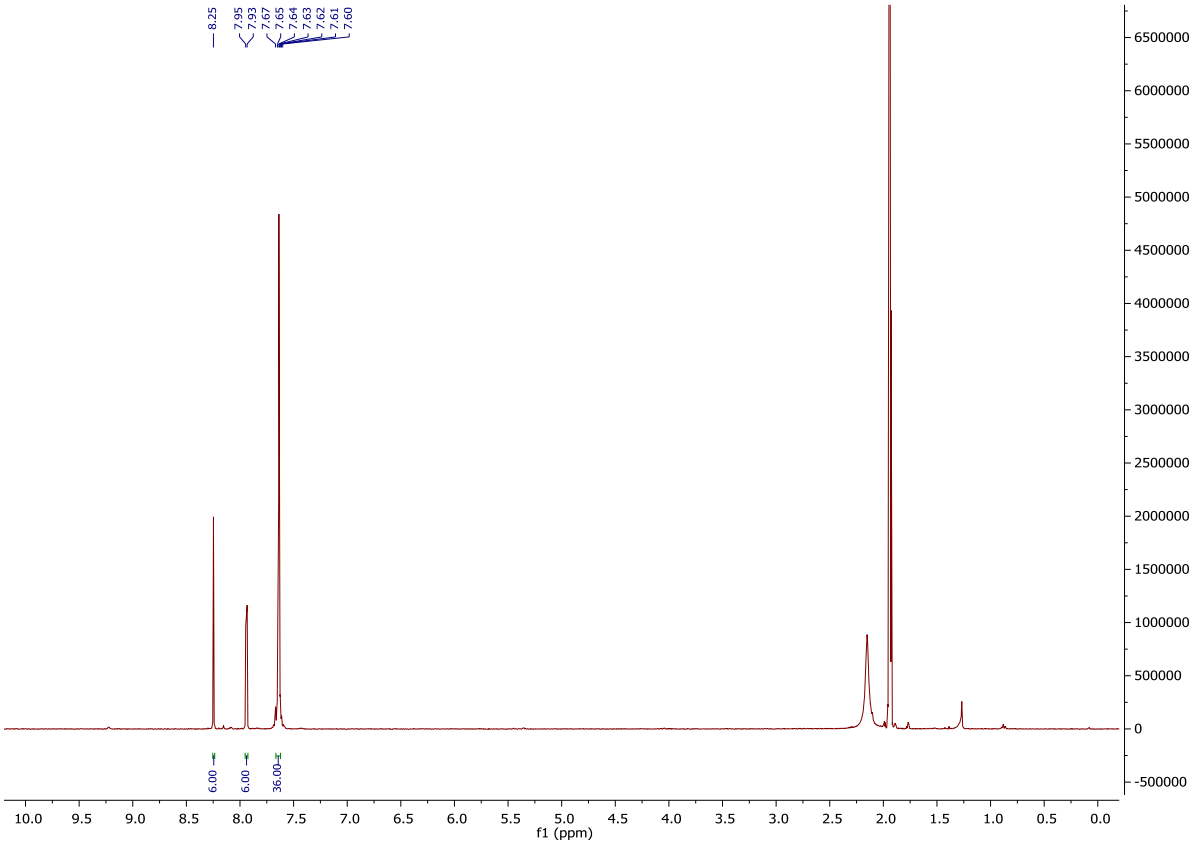

Figure S1. ^{1}H NMR spectrum of **4** in CD_3CN, 400 MHz.

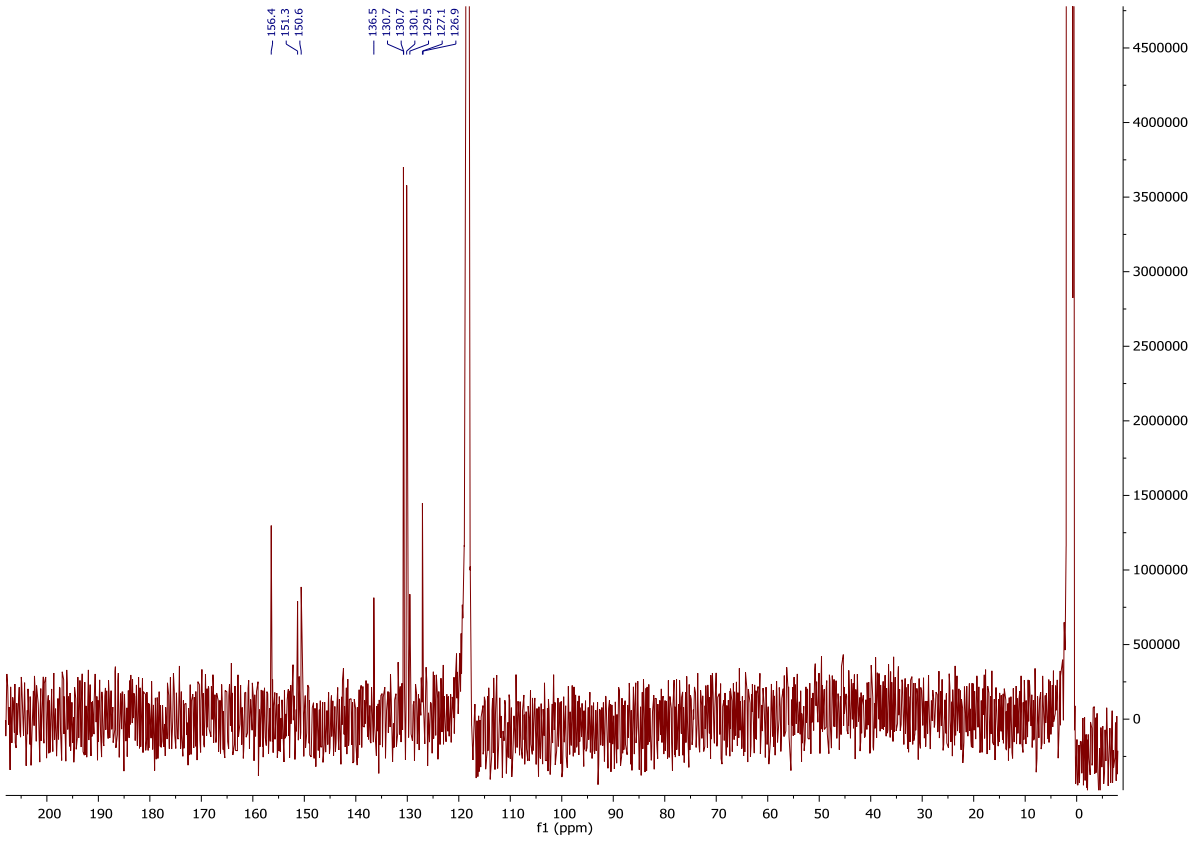

Figure S2. ^{13}C NMR spectrum of **4** in CD_3CN, 100 MHz.

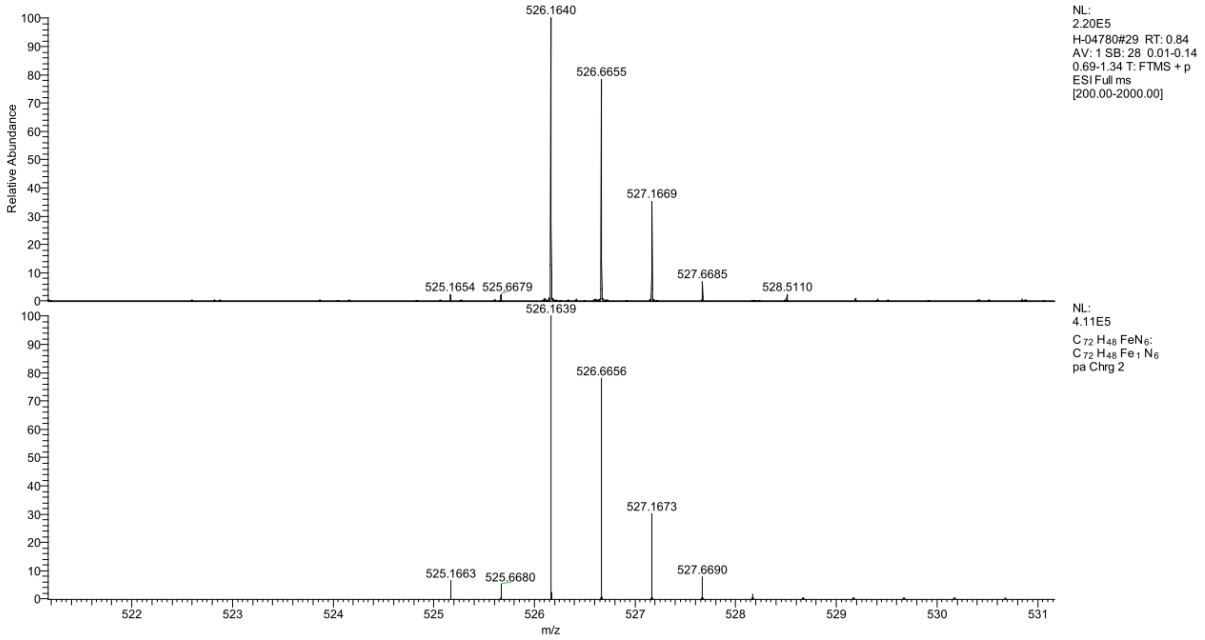

Figure S3. ESI-HRMS spectrum of **4** (positive detection mode).

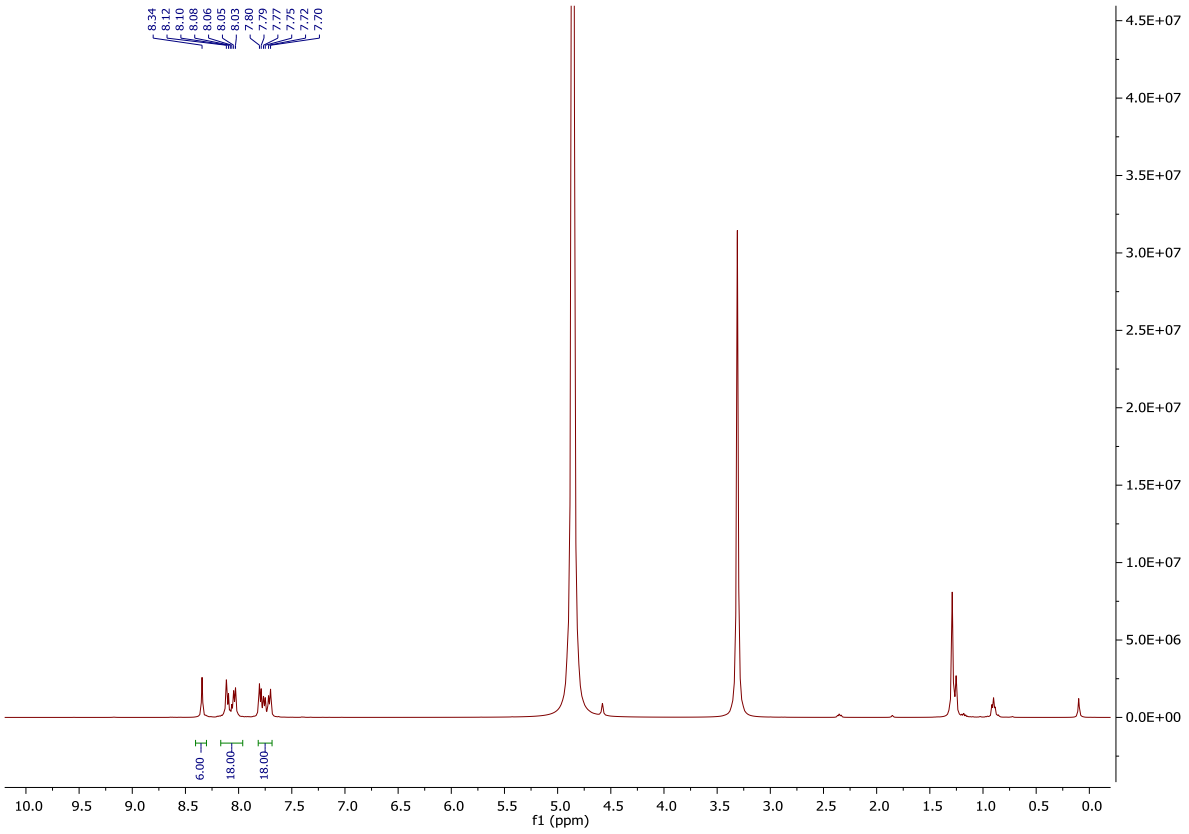

Figure S4. ^{1}H NMR spectrum of **5** in CD_3OD, 400 MHz.

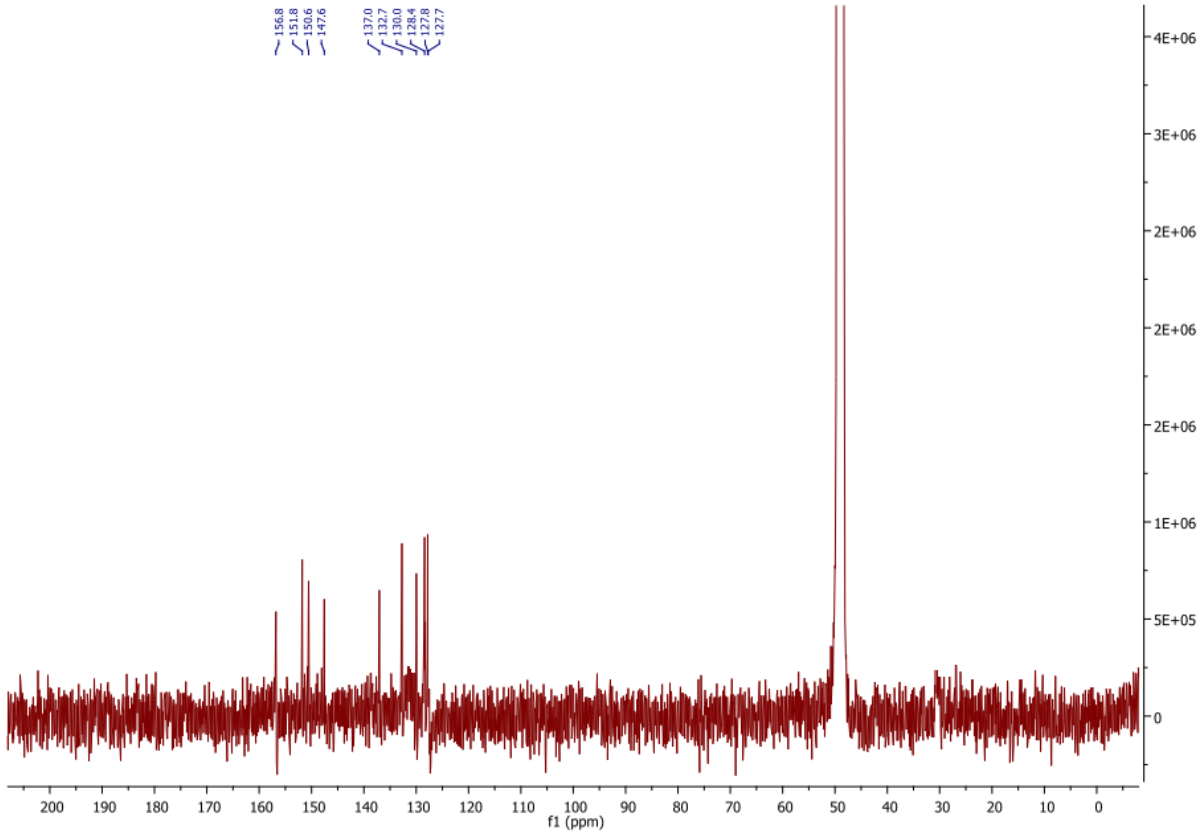

Figure S5. ^{13}C NMR spectrum of **5** in CD_3OD, 100 MHz.

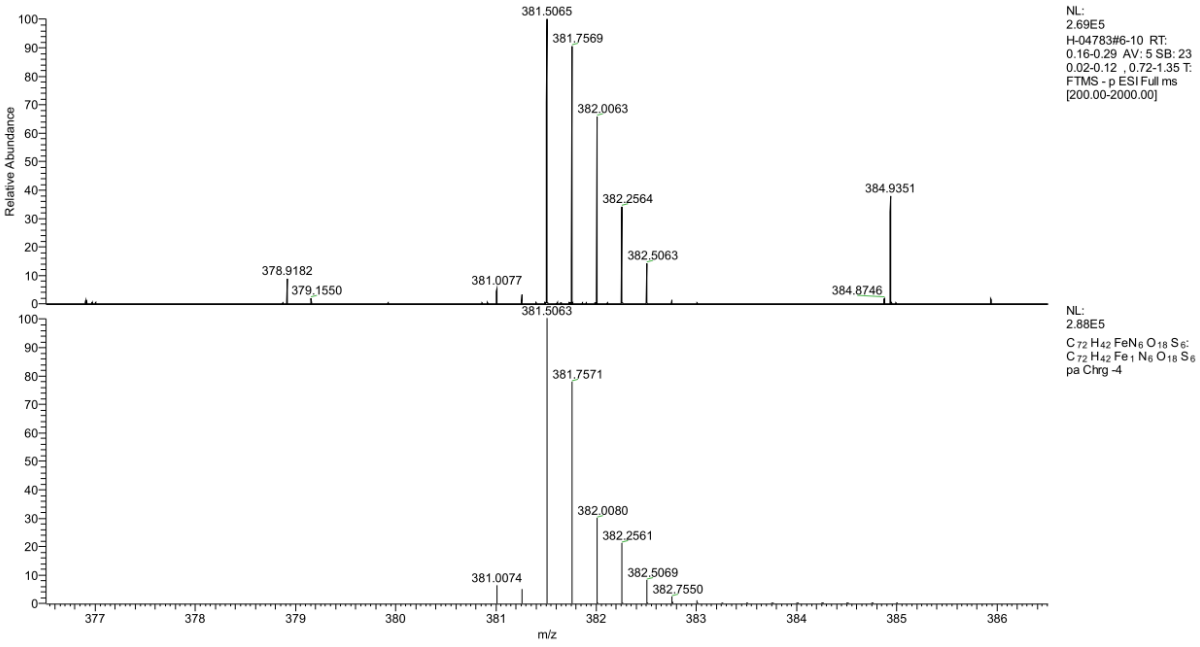

Figure S6. ESI-HRMS spectrum of **5** (negative detection mode).

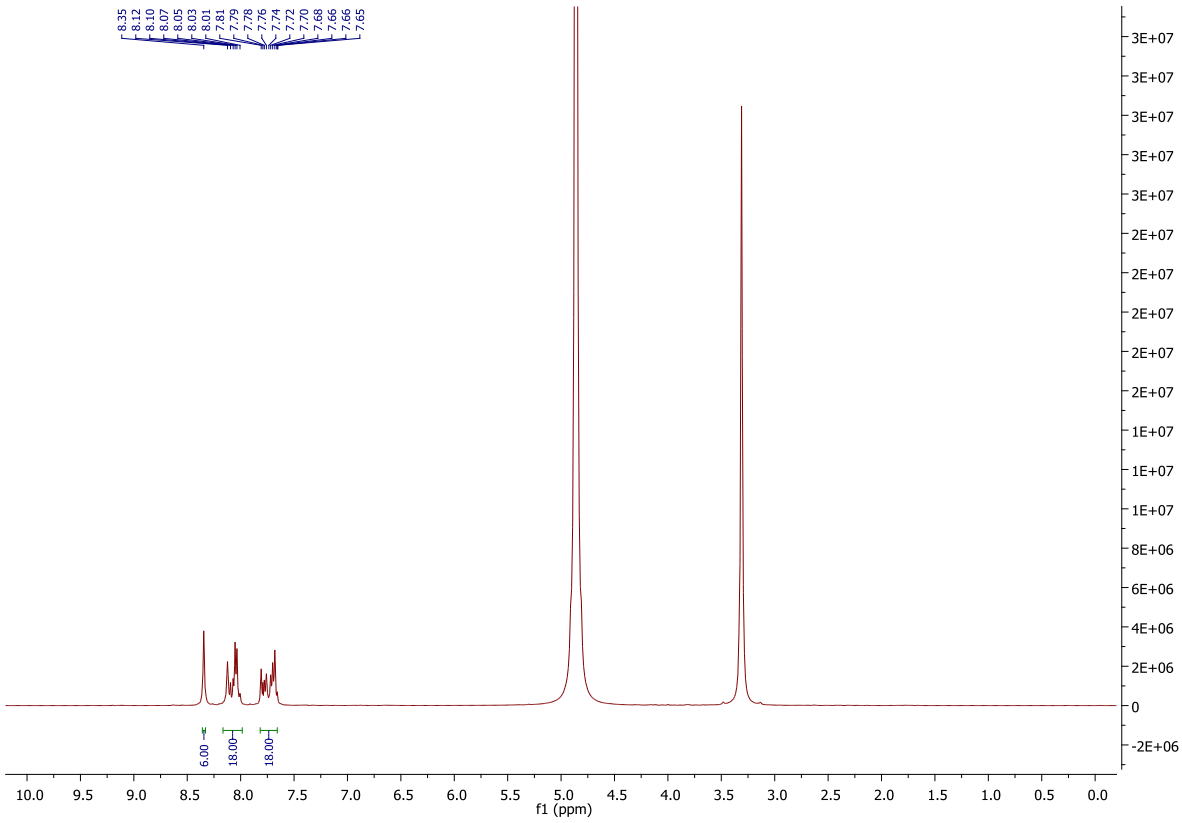

Figure S7. ^{1}H NMR spectrum of **6** in CD_3OD, 400 MHz.

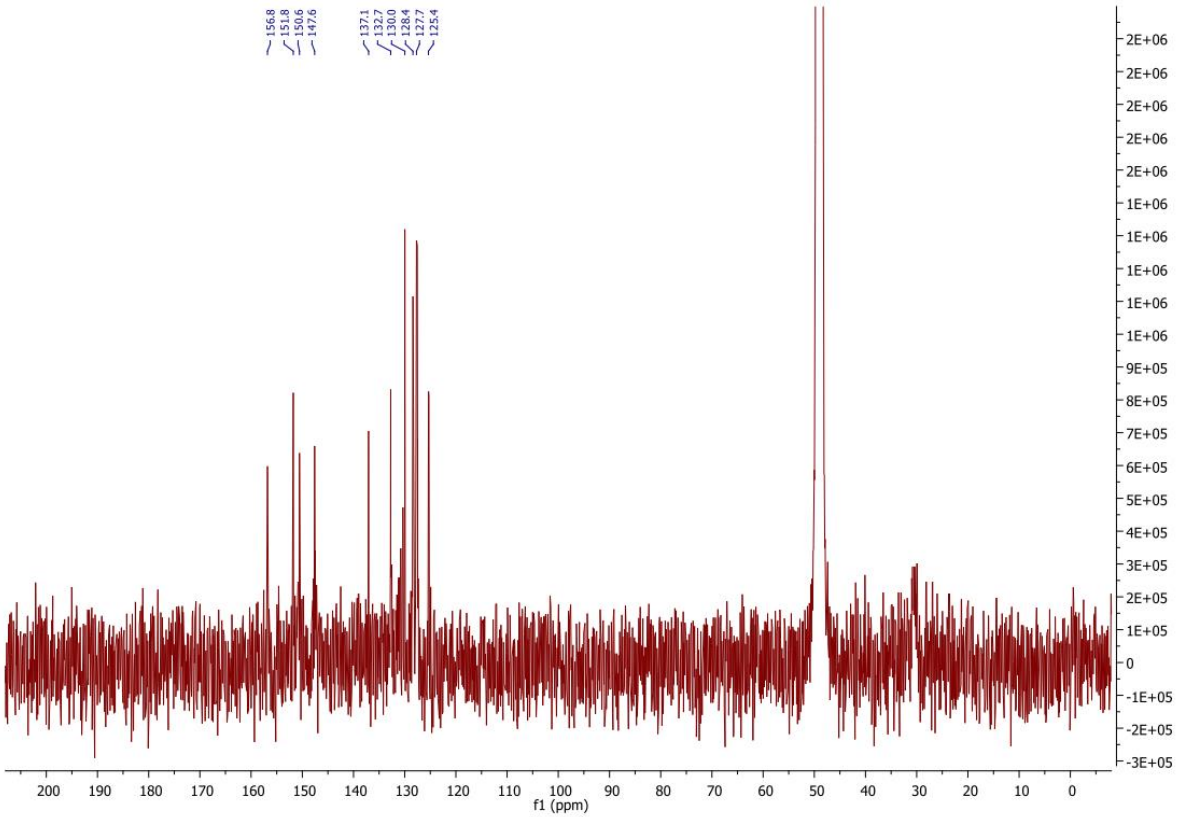

Figure S8. ^{13}C NMR spectrum of **6** in CD_3OD, 100 MHz.

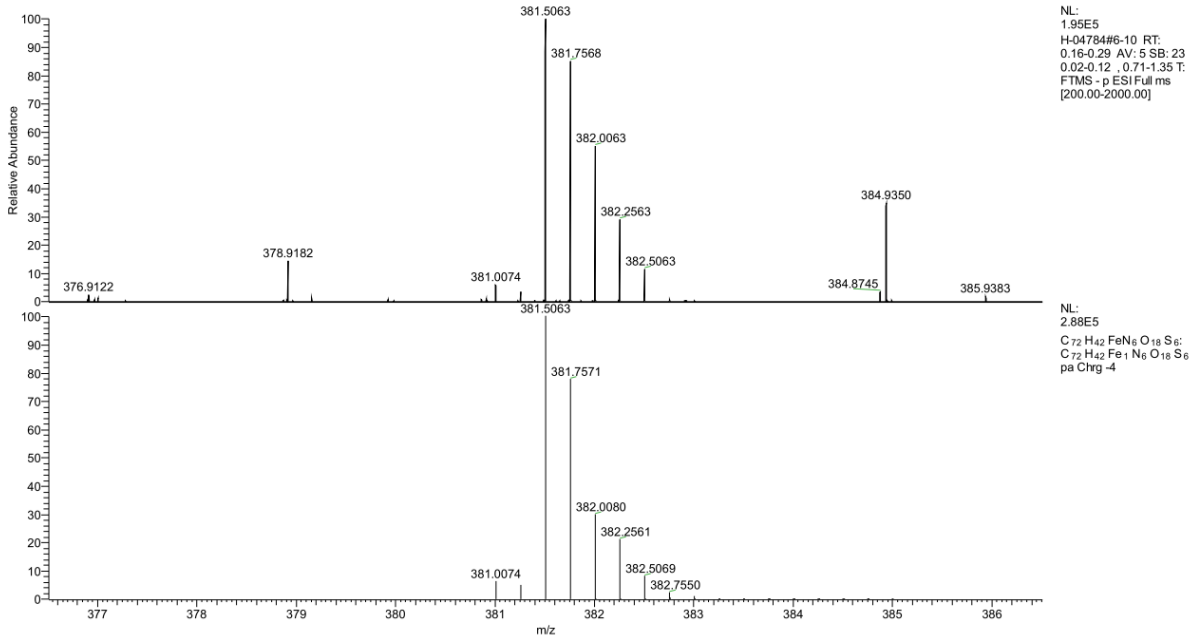

Figure S9. ESI-HRMS spectrum of **6** (negative detection mode).

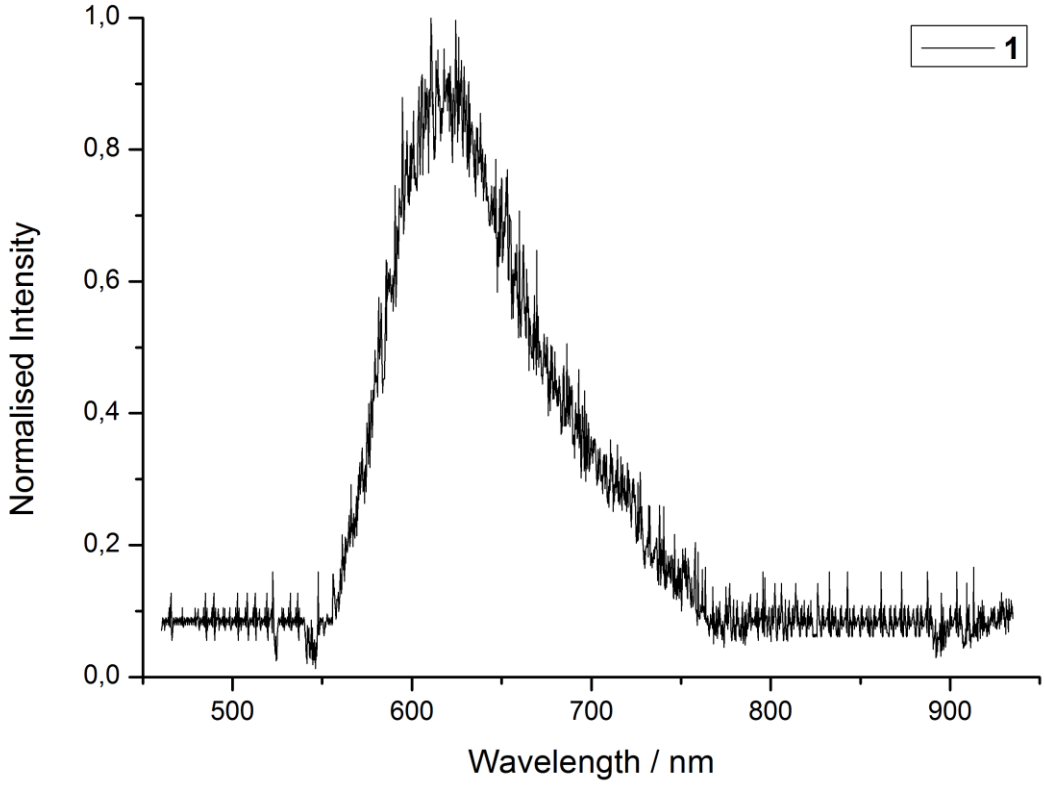

Figure S10. Normalised Emission Spectrum of **4** in CH_3CN.

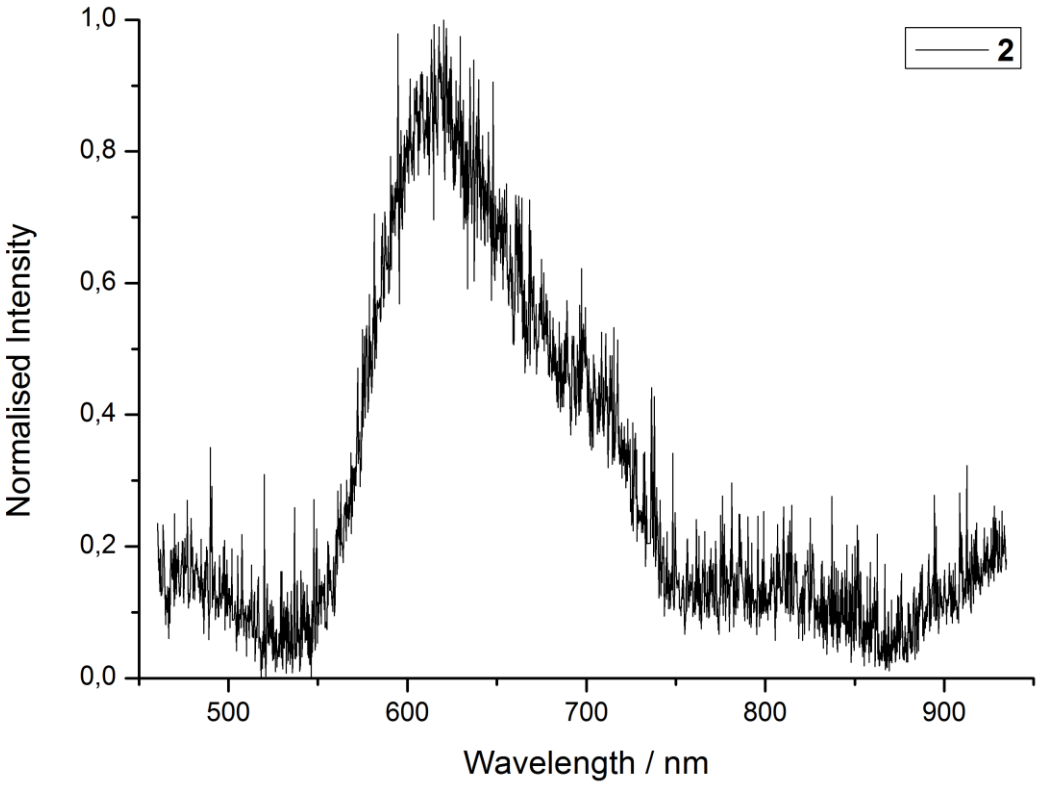

Figure S11. Normalised Emission Spectrum of **5** in CH_3CN.

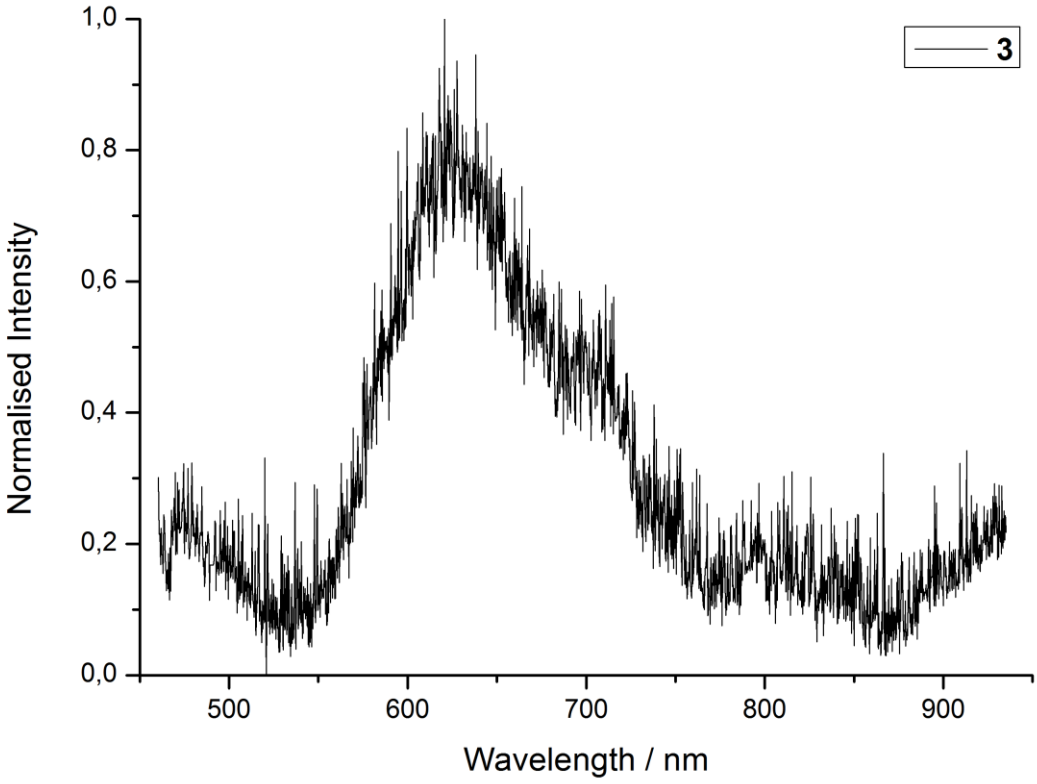

Figure S12. Normalised Emission Spectrum of **6** in CH_3CN.

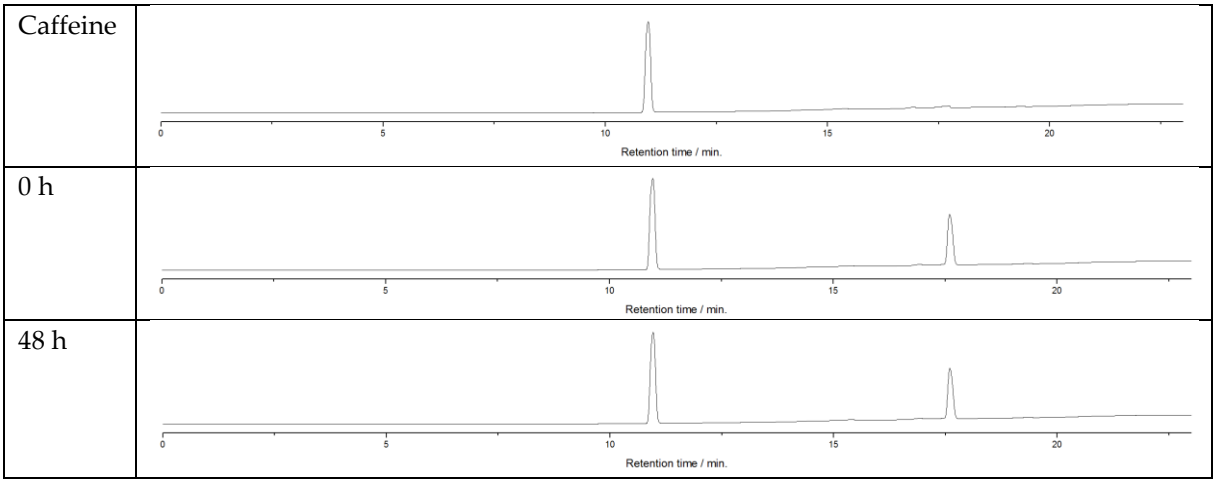

Figure S13. HPLC chromatogram of Caffeine (internal standard) and **4** after 0 and 48 h incubation in human pooled plasma.

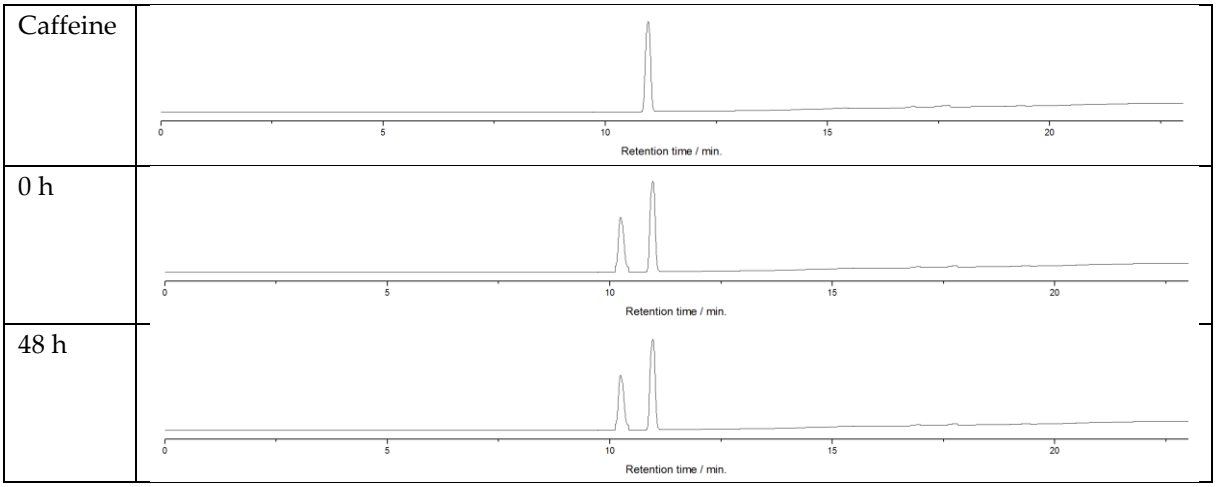

Figure S14. HPLC chromatogram of Caffeine (internal standard) and **5** after 0 and 48 h incubation in human pooled plasma.

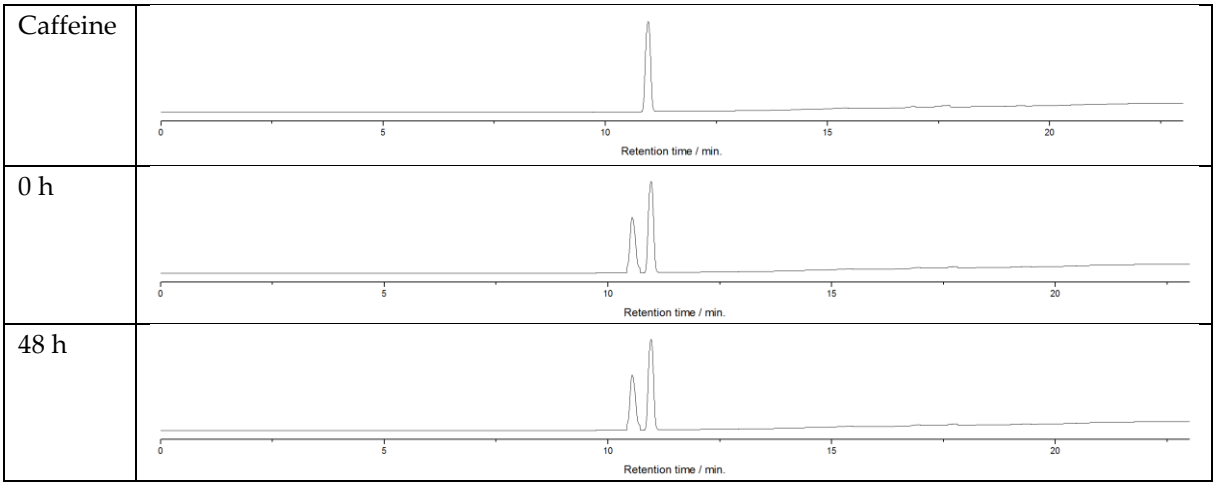

Figure S15. HPLC chromatogram of Caffeine (internal standard) and **6** after 0 and 48 h incubation in human pooled plasma.

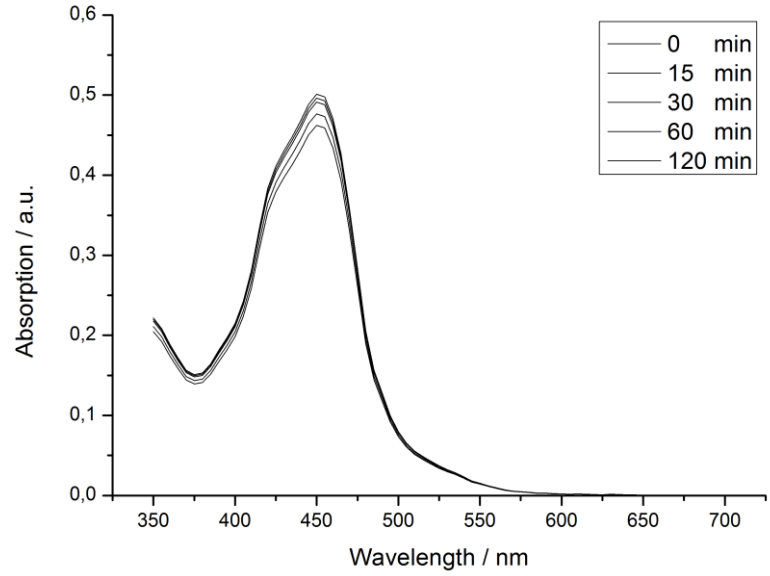

Figure S16. Temporal change of the UV/Vis spectra of $[Ru(bipy)_3]Cl_2$ by irradiation at 450 nm in CH_3CN.

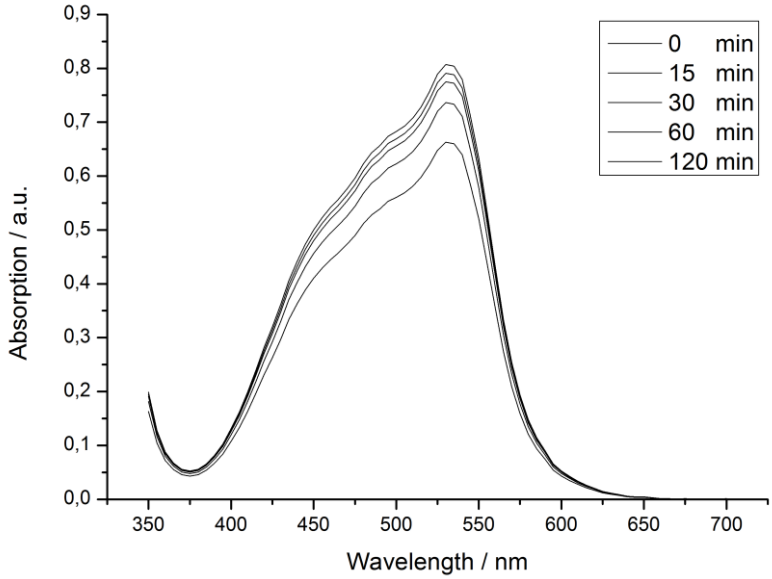

Figure S17. Temporal change of the UV/Vis spectra of **4** by irradiation at 450 nm in CH_3CN.

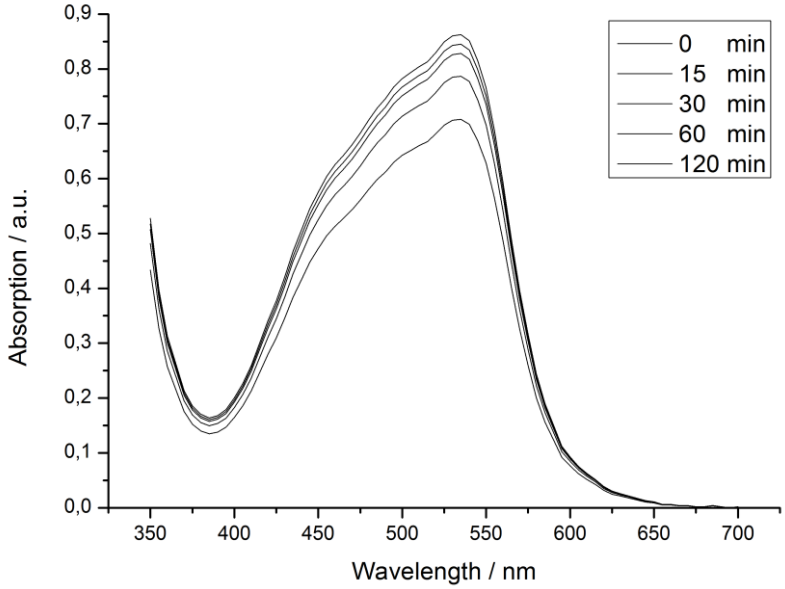

Figure S18. Temporal change of the UV/Vis spectra of **5** by irradiation at 450 nm in CH_3CN.

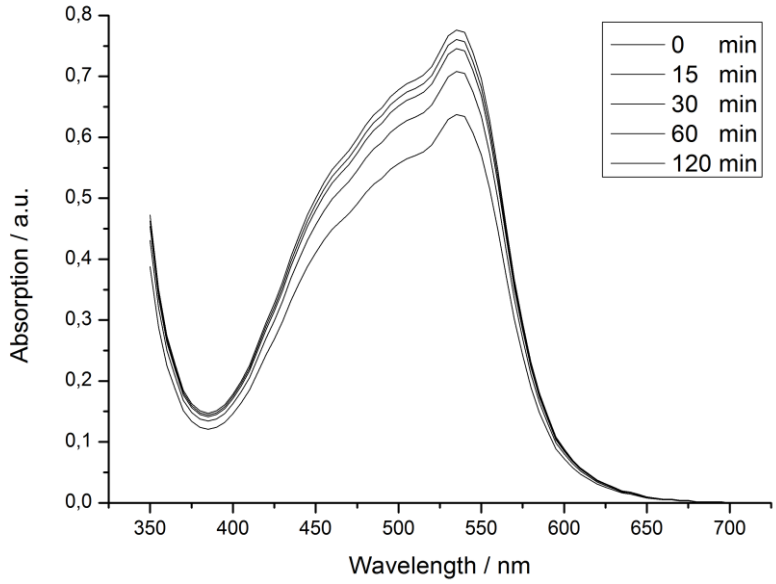

Figure S19. Temporal change of the UV/Vis spectra of **6** by irradiation at 450 nm in CH_3CN.

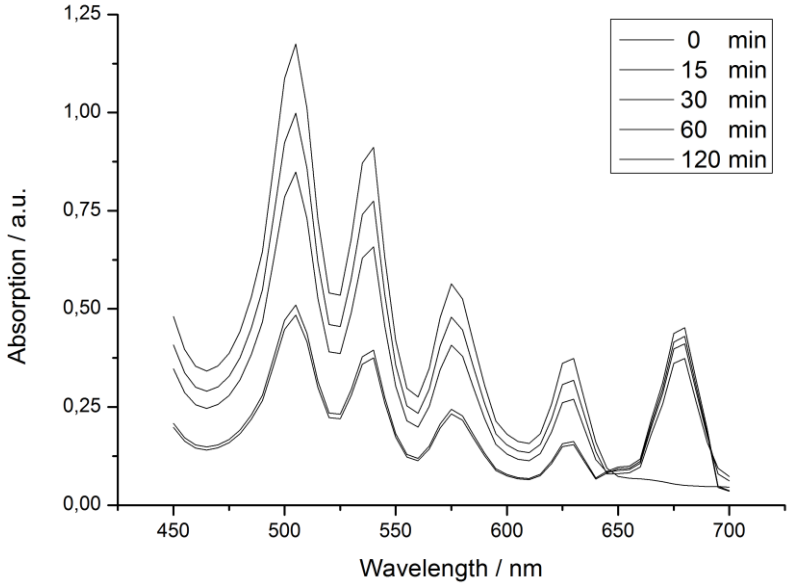

Figure S20. Temporal change of the UV/Vis spectra of PpIX by irradiation at 450 nm in CH_3CN.